JOURNAL OF CATALYSIS 81, 298–310 (1983)

Catalytic Properties of Defective Brannerite-Type Vanadates

I. Reactive Specificity of (20$\bar{2}$) and (201) Crystallographic Planes of $Mn_{1-x}\phi_xV_{2-2x}Mo_{2x}O_6$ in Oxidation of Propylene

JACEK ZIÓŁKOWSKI[1] AND JANUSZ JANAS

Institute of Catalysis and Surface Chemistry, Polish Academy of Sciences, ul. Niezapominajek, 30-239 Kraków, Poland

Received January 14, 1981; revised October 18, 1982

Oxidation of propylene in the presence of $Mn_{1-x}\phi_xV_{2-2x}Mo_{2x}O_6$ solid solutions ($0 \leq x \leq 0.3$, ϕ denotes a cation vacancy at the Mn^{2+} site) has been studied in an integral-flow system at 360–440°C over a wide range of contact time. Acrolein, acrylic acid, acetic acid, acetaldehyde, CO, and CO_2 were identified as the reaction products. Reactive specificity of the (20$\bar{2}$) and (201) crystallographic planes has been observed. The (20$\bar{2}$) plane is much more active and characterized by at least two types of active centers (yielding C_3 and C_2/C_1 products) able to incorporate, without desorption, more than one oxygen atom into the molecule of propylene or into the products of its degradation. On the contrary, on the (201) plane predominate centers capable of the successive, one by one, incorporation of oxygen into the organic molecule, separated by desorption–adsorption processes. A common feature of both planes is that the total combustion markedly diminishes with the increase of the composition parameter x. Detailed schemes of the reaction on both crystallographic planes are proposed and discussed.

INTRODUCTION

Oxide solid solutions have been frequently used as model catalysts for oxidation reactions. Their advantage consists in the possibility of controlled and fluent change of the selected parameter believed to be responsible for catalytic properties (e.g., the kind and concentration of dopant or various defects) with conservation of other parameters at a fixed level (structure of the matrix and all related properties). An excellent review of these possibilities has been given by Stone (*1*). Until now, however, most studies have dealt with binary oxide solid solutions of ionic lattices catalyzing simple reactions such as CO oxidation and N_2O decomposition. This fact has limited the diversity of catalytic studies. Recently, Sleight and co-workers (*2*) have demonstrated that the scheelite structure offering a wide variety of chemistry is very useful in fundamental studies of the mechanism of isomerization, oxidation, and ammoxidation of olefins. The careful choice of scheelite-type samples of different composition (e.g., $Pb_{1-3x}Bi_{2x}\phi_xMoO_4$, $Pb_{1-3x}La_{2x}\phi_xMoO_4$, $Pb_{1-2x}Bi_xNa_xMoO_4$) enabled these authors to recognize the difference between the role of bismuth, cation vacancies (ϕ), and the electronic factor in the above reactions.

In developing the abovementioned ideas we decided to inspect the brannerite-type phases as model catalysts for oxidation of olefins.

The brannerite ($ThTi_2O_6$) structure, which can be generally formulated as AB_2O_6, is monoclinic with the space group $C2/m$. Both A and B cations are octahedrally coordinated by six oxygen atoms. BO_6 octahedra, sharing three edges, form anionic sheets parallel to the (001) plane. A atoms, binding these sheets together, are

[1] To whom correspondence should be addressed.

0021-9517/83 $3.00

located in AO_6 octahedra, joined by two edges and forming chains along the *b*-axis. A detailed description of the structure is given in the literature (*3–5*). The structure is amenable to the substitution of other cations provided that only the charge balance is fulfilled ($A^{IV}B_2^{IV}O_6$, $A^{II}B_2^{V}O_6$, $A^{I}B^{V}B''^{VI}O_6$. Among others, a number of divalent metal vanadates (A = Mg, Co, Cd, Hg, Zn, Mn) also adopt the brannerite or brannerite-related (Cu) structure (*4, 6–9*).

As we have pointed out in recent papers (*5, 10, 11*) one may introduce into the brannerite-type vanadates ion combinations which give rise to cation vacancies at the A sites. The following solid solutions have been identified so far: $M_{1-x}\phi_xV_{1-x}Mo_{1+x}O_6$ (M = Li, $0 \le x \le 0.16$; M = Na, $0 \le x \le 0.30$; M = K, $0.18 \le x \le 0.24$; M = Ag, $0 \le x \le 0.12$) (*12*); $Mn_{1-x}\phi_xV_{2-2x}Mo_{2x}O_6$ ($0 \le x \le 0.45$) (*5, 10*); $Cu^{2+}_{1-x-y}Cu_y^{1+}\phi_xV_{2-2x-y}Mo_{2x+y}O_6$ ($x_{min} = y_{min} = 0$, $x_{max} = 0.23$, $y_{max} = 0.27$) (*11*) and $Zn_{1-x}\phi_xV_{2-2x}Mo_{2x}O_6$ ($0 \le x \le 0.12$) (*13*). This variety of chemistry in the brannerite-type vanadates has encouraged us to use them as model catalysts.

The original aim of the present work was to study the effect of increasing concentration of Mo and ϕ in $Mn_{1-x}\phi_xV_{2-2x}Mo_{2x}O_6$ (designated MV–X, where X = 100*x*) solid solutions on the mechanism of the oxidation of propylene. Unexpectedly a reactive specificity of (20$\bar{2}$) and (201) crystalline faces of MV-X has been observed and this interesting effect, similar to that already observed in other systems (*14, 15*), has become one of the main points of this paper.

EXPERIMENTAL

All MV-X catalysts were prepared by high temperature calcination (see Table 1) of the respective mixtures of Mn_2O_3, V_2O_5, and MoO_3 and checked by X-ray analysis and DTA as described in detail elsewhere (*5*). The X-ray and DTA patterns of the samples were the same before and after catalytic testing. The BET (low temperature Kr adsorption) surface area of the catalysts amounted to 0.3–0.7 m^2/g and the exact values were used to calculate the contact time τ (see below). Scanning electron microscopy observations were carried out in a JEOL JXA-50A instrument at a magnification of 3000–20,000×.

TABLE 1

Conditions of Preparation of MV-X Catalysts

X	0	10	15	20	30	35
Calcination conditions[a]	H	S_2	S_3	H	H	H

[a] The data pertain to samples used in preliminary catalytic testing. Mn_2O_3, V_2O_5, and MoO_3 were weighed in appropriate proportions and ground together. S_2 and S_3 indicate stepwise calcination of the initial mixture for 20 h consecutively 2 × 520, 540, 560, 580 and 3 × 600°C (S_2) and 2 × 520, 540, 560, 580, and 600°C (S_3). H indicates calcination at 600°C twice for 20 h. After each step of 20 h calcination samples were cooled and ground. These conditions were elaborated experimentally and corroborated on the basis of the determined reaction mechanism (*10*) and MnV_2O_6–MoO_3 phase diagram (*5*). The oxides Mn_2O_3, V_2O_5, and MoO_3 coming from various factories or from various batches differ in grain size and grain distribution and consequently in solid state reactivity. If the reactivity is high the entire conversion may be reached before the last step of 20 h calcination. If it is low, one or two additional steps of calcination at 600°C for 20 h are necessary to complete the reaction. At the same time, the morphology of the final product changes. However, factors influencing the morphology remain at present beyond rational control. As follows from our preliminary observations, the higher the temperature and the longer the time of annealing, the larger the contribution of the (201) face which is evidently the face of lowest surface energy. Changing the preparation conditions in the above-indicated limits we have produced a large number of MV-X preparations of various factors *f*. Of this set, the samples of (201) series ($1.8 < f < 2.0$) and of (20$\bar{2}$) series ($1.2 < f < 1.4$) were selected.

Catalyst testing was performed in a single-pass integral flow system, operating at atmospheric pressure, at 360–440°C in a wide range of contact time. The reactor consisted of two connected tube-in-tube vertical parts 250 mm long and 10 or 14 mm i.d. for the inner tube. The upstream gas being heated to a desired temperature

served simultaneously as a temperature profile agent. The temperature of the catalyst bed was maintained within ±1°C of the required value and controlled by a thermocouple localized centrally in the reactor. About 2.5 g (2 cm^3) of the catalyst (64–144 mesh) was placed into the reactor upon a layer of 1–2 cm^3 of pyrex glass powder (144–196 mesh) to minimize the catalyst loss. Commercial, research grade, propylene and oxygen passed through a silica-gel tower were used as reactant gases. The typical composition of the feed gas was 7–10 vol% of propylene and 90–93 vol% of oxygen and its flow rate was 30–200 cm^3/min. The "contact time" τ, expressed as reciprocal volume flow rate (V), normalized to the total surface area of the catalyst (A), was calculated from the formula:

$$\tau = \frac{AT_f}{VT_r\left(1 - \frac{20}{760}\right)} \quad \left(\frac{m^2 s}{cm^3}\right)$$

comprising the pressure correction of the soap film flowmeter and the correction for the temperature difference between the flowmeter (T_f) and the reactor (T_r).

In each case the catalyst was heated up in the stream of reactants and kept at the desired temperature to attain steady-state conditions (usually 1–2 h) which were then held for at least 3 h.

The composition of the gas mixture was determined by gas chromatography. The gases entering and leaving the reactor passed through a sampling system. A conventional six-way valve fed the effluent gases to an FID part which consisted of a 2 m × 3 mm i.d. column filled with 2 wt% DEGA and 4 wt% Carbowax 20M on AW Chromosorb W (for separation and analysis of liquids, e.g., aldehydes, acids). Rotating-loop three-position valves fed reactants or effluent gases to a TCD part which consisted of a 4 m × 3 mm i.d. column filled with 15 wt% DMS on AW Chromosorb P (for separation and analysis of C_3H_6 and CO_2) and a 1 m × 3 mm i.d. column filled with 13× molecular sieves for analyzing O_2 and CO. A 1 m column filled with Porapak T and operating in a back-flush system was used for protecting the latter-mentioned column from contamination by water and other products. All the chromatographic columns were made of stainless steel. The carrier gases (He for TCD analysis and N_2 for FID analysis) were supplied from commercial cylinders.

Homogeneous reactions were negligible as found experimentally using a reactor filled with pyrex glass powder instead of catalyst. To minimize possible heterohomogeneous reactions the postcatalytic volume was reduced as far as possible.

The reaction products were composed usually of acrolein and acrylic acid (C_3), acetic acid and acetaldehyde (C_2), CO and CO_2 (C_1). These six products gave a balance with the propylene consumed within ±5%. Sometimes propionaldehyde, benzene, or formic acid appeared in trace amounts. Conversion [Conv = (propylene consumed)/(propylene introduced)], yield of i-product [Y_i = (propylene transformed to i)/(propylene introduced)] and selectivity ($S_i = Y_i$/Conv) were calculated in the standard manner. The experimental results, described in detail below, suggested that C_2 products are formed as a result of double bond breaking, the CH_3—CH= species being transformed to acetic acid or aldehyde and CH_2= species undergoing combustion. To distinguish between C_1 products formed in this manner and those appearing due to the consecutive oxidation of C_2 and C_3 products or "one stage combustion" of propylene (see below) and thus to evaluate the probability of different reaction paths a "selectivity" σ has been calculated as $\sigma_3 = S_3$, $\sigma_2 = \frac{3}{2} S_2$, $\sigma_1 = 100\text{-}\sigma_3\text{-}\sigma_2$ where the indexes denote C_1, C_2, and C_3 products, respectively. In other words, S_2 and σ_2 express the selectivity of the reactions: 2 $C_3H_6 \rightarrow 3\ C_2$ and $C_3H_6 \rightarrow C_2 + C_1$, respectively. Initial selectivities σ_1^0, σ_2^0, and σ_3^0 were also determined by extrapolating the σ–τ curves to $\tau = 0$.

RESULTS AND DISCUSSION

Preliminary Catalytic Testing

Preliminary catalytic testing was performed for MV-0, MV-15, MV-20, MV-30, and MV-35 samples at 360, 400, and 440°C and at a feed gas flow rate of 60 cm^3/min. Small differences in the surface area of this series of preparations were neglected; the contact time was about 0.6. Representative results in conversion vs x and S vs x coordinates obtained at 400°C are presented in Fig. 1. Unexpectedly, the experimental curves expressing the dependence of catalytic activity and selectivity on the composition parameter x passed over several extrema. This unusual fact was explained when the catalytic specificity of different crystalline faces of MV-X solid solutions was recognized. As is evident from Fig. 1 the catalytic properties of the series of samples are ruled by a morphological factor f expressing (in arbitrary units) the ratio of the contribution of (201) and ($20\bar{2}$) planes in the external surface of the grains of catalysts. The meaning of f will be discussed in detail below. The higher the value of f the higher is S_3 and the lower are the conversion and S_1. This last conclusion has been confirmed in an additional experiment in which the catalytic properties were compared for two preparations of the same

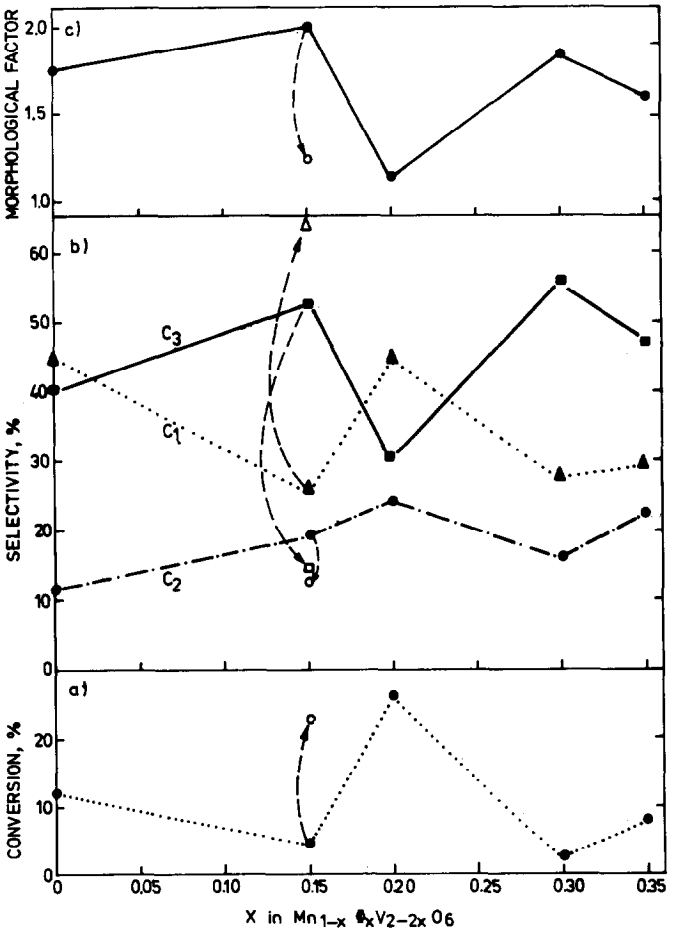

FIG. 1. Preliminary testing of $Mn_{1-x}\phi_xV_{2-2x}Mo_{2x}O_6$ (MV-X) solid solutions in oxidation of propylene at 400°C: (a) conversion vs composition, (b) selectivity S vs. composition, and (c) morphological factor f vs composition. Arrows to the open points show the changes in conversion and selectivity of MV-15 when f is decreased as shown in (c).

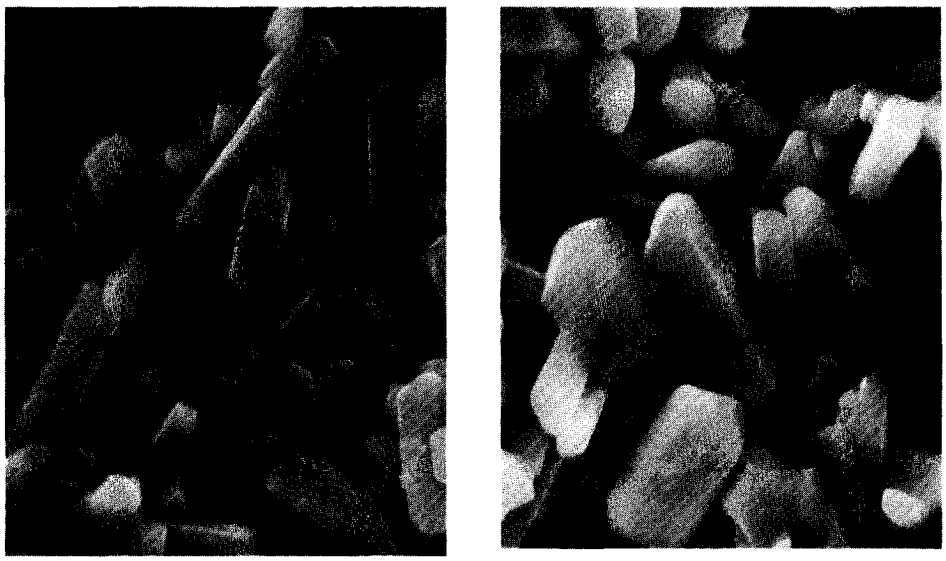

FIG. 2. Typical grain shapes of the MV-X catalysts as observed by scanning electron microscopy (×4000): left, elongated bars prevailing in the (20$\bar{2}$) series; right, plates prevailing in the (201) series.

composition (MV-15) but of different values of f. The results of this experiment are included in Fig. 1.

Morphological Factor

As follows from scanning electron microscopy observations (Fig. 2), the grains of powder samples of MV-X solid solutions are of a shape varying between elongated thin plates and elongated bars of nearly rectangular section. This suggests that the external surface of the grains consists mainly of two practically perpendicular crystallographic planes. When pressed in the X-ray sample-holder the laminar grains become oriented and this brings about a strong change in the intensity of some X-ray reflections as compared with the calculated values or with experimental ones determined with a special technique ensuring an entirely unoriented sample layer[2] (*5*). In this manner (201) and (20$\bar{2}$) planes, making an angle of about 84° in the MnV_2O_6 structure were identified as the external planes exposed by the grains. This conclusion is consistent with the observation of Kozłowski and Stadnicka (*16*) who found that monocrystals of MV-X solid solution grown from the melt are of thin-plate shape with a large face corresponding to the (201) crystallographic plane.

A morphological factor f defined as:

$$f = \frac{I_{201}}{I_{20\bar{2}}}$$

was thus taken as a semiquantitative measure of the contribution of the respective planes in the external surface of the grains. I in the above formula denotes the intensity of the X-ray reflection measured for the oriented sample, prepared by standard pressing (smoothing) in the X-ray sample-holder. In practice, f was determined for each sample at least three times and the reproducibility of the results was within ±3%. No change of f value was observed after the catalytic testing. Theoretically the $I_{201}/I_{20\bar{2}}$ ratio equals 1.14 ± 0.02 independently of x in $Mn_{1-x}\phi_xV_{2-2x}Mo_{2x}O_6$ formula (*5*). The experimental values obtained for unori-

[2] This technique included passing the ground powder through a 400 mesh screen placed over a flat quartz sample-holder covered with paraffin oil. The grains fall down and adhere to the plate producing an entirely unoriented sample layer.

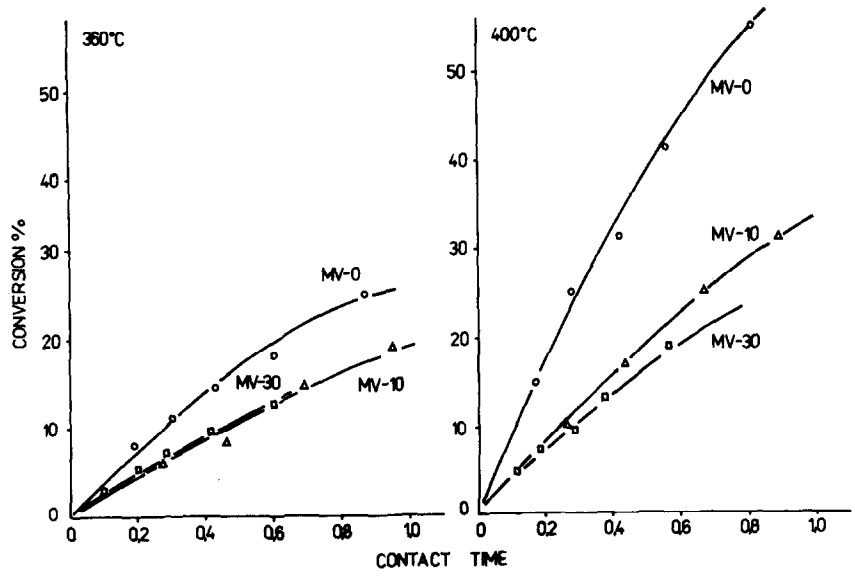

FIG. 3. $(20\bar{2})$ series of MV-X. Conversion vs contact time.

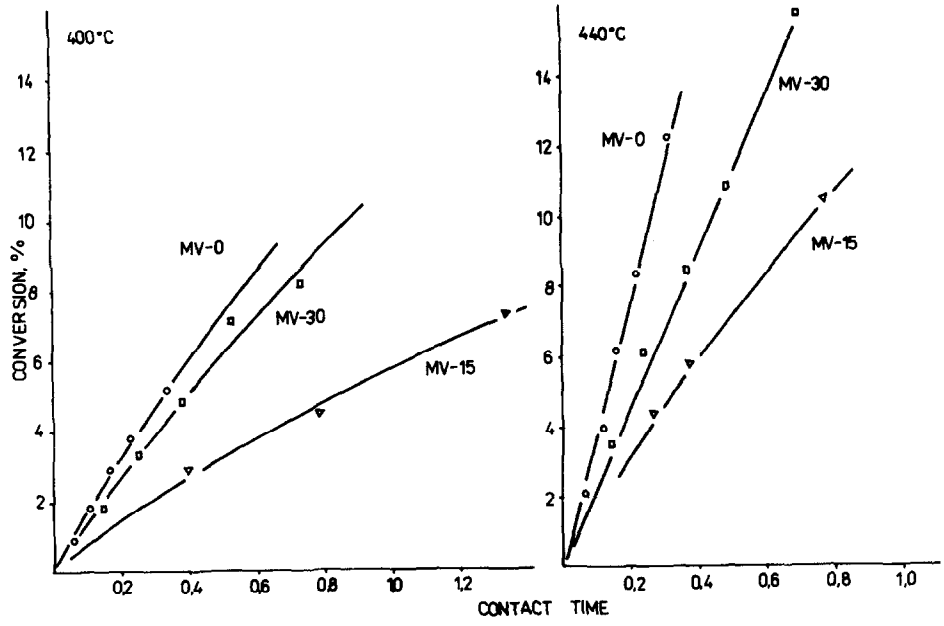

FIG. 4. (201) series of MV-X. Conversion vs contact time.

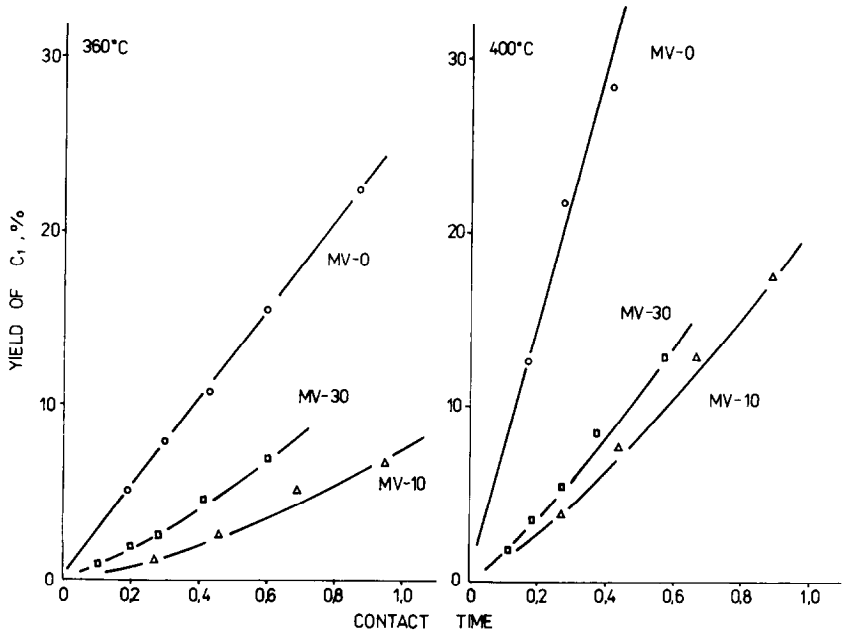

FIG. 5. (20$\bar{2}$) series of MV-X. Yield of C_1 products as a function of contact time.

ented samples are very close to this. The f factors for the oriented samples vary over a wide range depending on the synthesis conditions.

For the purpose of further studies two series of preparations were selected (see Table 1). The first one, labelled as (201), comprised the samples of composition of MV-0, MV-15, and MV-30 and with f values between 1.8 and 2.0. The second series, labeled as (20$\bar{2}$), included MV-0, MV-10, MV-15, MV-20, and MV-30 with f between 1.2 and 1.4. Such a choice of samples enabled us to identify the differences between the mechanism of oxidation of propylene on the two faces and to determine the influence of composition (x) on the mechanism. It should be mentioned that the contribution of the two planes under discussion in the external surface of the (20$\bar{2}$) series was comparable. However, due to the much higher catalytic activity of the (20$\bar{2}$) plane as compared to the (201) plane the results obtained for the (20$\bar{2}$) series may be regarded as sufficiently representative for the (20$\bar{2}$) plane only.

(20$\bar{2}$) *Series of MV-X Catalysts*

Figures 3, 5, and 6 present the dependence of the conversion of propylene and the yield of C_1, C_2, and C_3 products on contact time for the catalysts of the (20$\bar{2}$) series as measured at 360 and 400°C. As seen in Fig. 3, MV-0 is the most active sample of the series. On passing to MV-10 the activity falls strongly and with further increase of x it changes insignificantly. Due to this fact and for the sake of clarity in the figures the results for MV-15 and MV-20 are omitted. As is evident from Figs. 5 and 6 an important decrease of Y_1 is mainly responsible for the abovementioned change in activity. On the contrary, Y_3 and Y_2 increase with x and pass over a more or less marked maximum at MV-10.

Figure 8 presents the $Y-\tau$ curves for all six reaction products as determined for MV-10 at 400°C, the results being representative in many respects for whole (20$\bar{2}$) series. At low contact time acrolein is the main reaction product. Its $Y-\tau$ curve shows a strong monotonic decrease of the deriva-

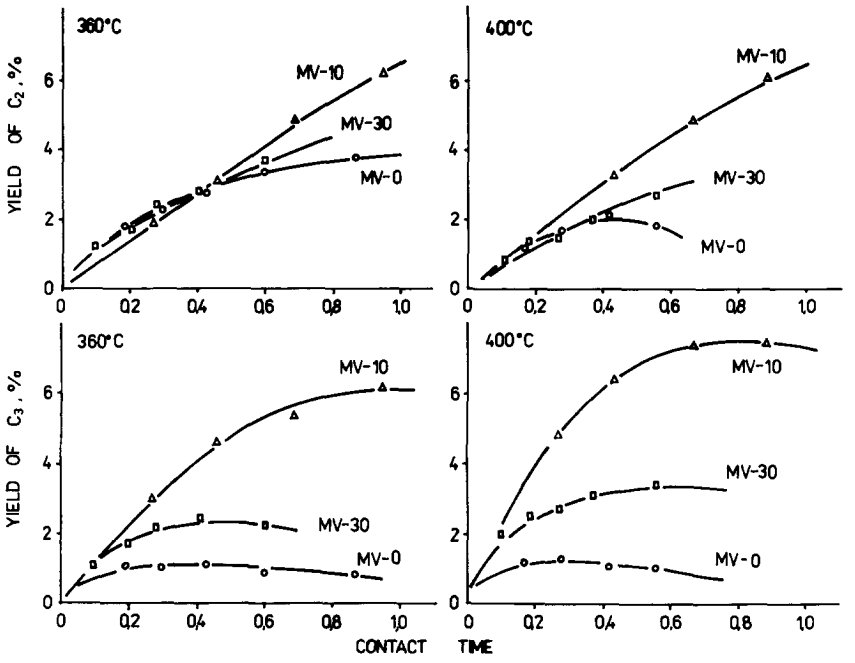

FIG. 6. (20$\bar{2}$) series of MV-X. Yield of C_2 and C_3 products as function of contact time.

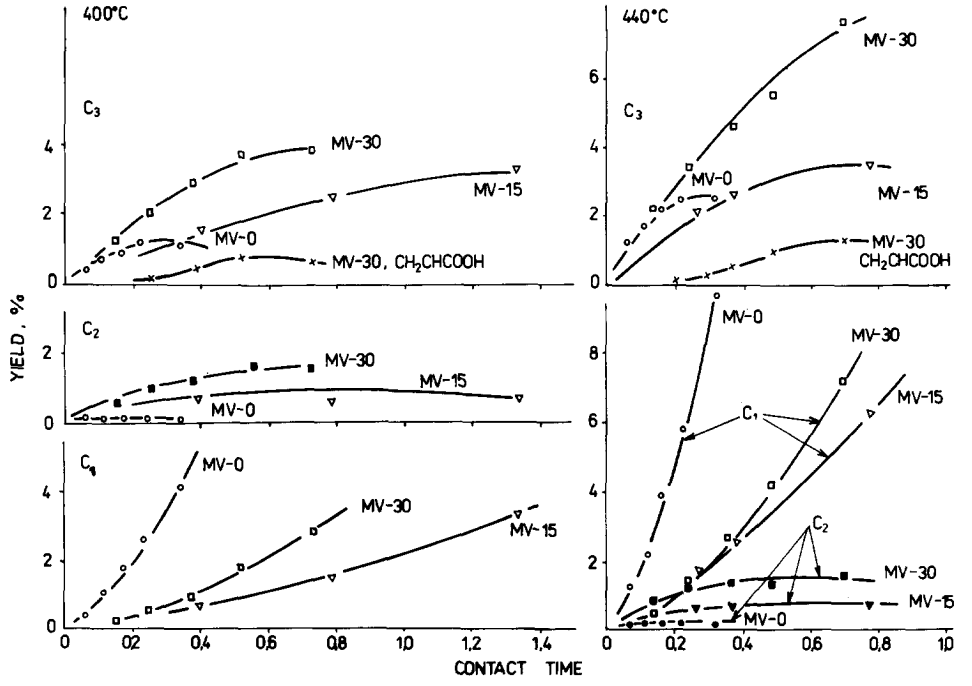

FIG. 7. (201) series of MV-X. Yield of C_1, C_2, and C_3 products as a function of contact time. As an example, Y–τ curves for acrylic acid over MV-30 are included, proving that it is formed and consumed in the consecutive reactions. The Y–τ curves for acrylic acid over MV-15 as well as those for acetic acid on both catalysts are of analogous shape.

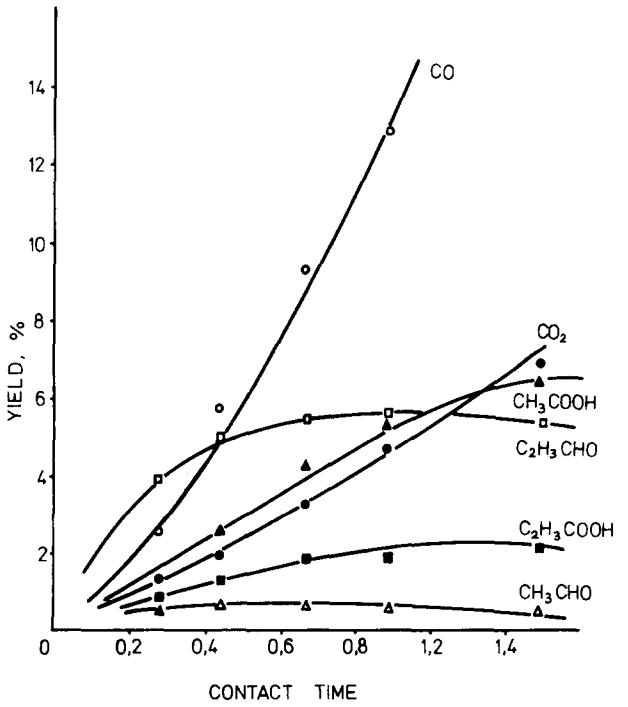

FIG. 8. Yield vs contact time for all six reaction products as measured at 400°C for MV-10 belonging to the $(20\bar{2})$ series of MV-X.

tive proving that acrolein is consumed in a consecutive reaction. As the increment of the acrylic yield does not compensate that decrease, one may conclude that acrolein is consecutively combusted. The yield of acrylic acid is small compared to acrolein, apart from the fact that for MV-10 it is the highest in the whole $(20\bar{2})$ series.

The $Y-\tau$ curve for acetic acid is nearly linear, proving that we deal here with a directly formed and practically final product of the reaction. Solely in the presence of MV-0 is acetic acid combusted in the consecutive reaction (see Fig. 6). Acetaldehyde is always formed in very small amounts and its $Y-\tau$ curve is less informative.

C_1 products: CO_2 and CO are usually formed in a ratio close to 2:5. Their $Y-\tau$ curves show a systematic increase of the derivative, this fact being in agreement with the consecutive combustion of some products of partial oxidation (mainly acrolein).

We draw attention to Figs. 5, 6, 9, and 10 to analyze the dependence of the yield and selectivity to the different reaction products not only on τ but also on the temperature. Y_2 is proportional to τ, σ_2 is nearly τ-independent (exception made by MV-0), but they both distinctly decrease with temperature. As the consecutive combustion may not be a cause of this effect one may suppose that active complexes formed on the active center K_2 (see Fig. 12a) may decompose alternatively to acetic acid (and acetaldehyde) or directly to C_1 products, the probability of the second of these reaction paths being increased with temperature. Actually, the selectivity $\sigma_1^0 > 0$. This means that C_1 products are not only formed in the consecutive reaction but also as if in a one-stage reaction. The characteristic feature of the K_2 active centers should therefore be the simultaneous attack of several atoms of oxygen on the molecule of propylene, particularly on its double bond.

As concerns the oxidation of propylene to acrolein and acrylic acid, the mechanism

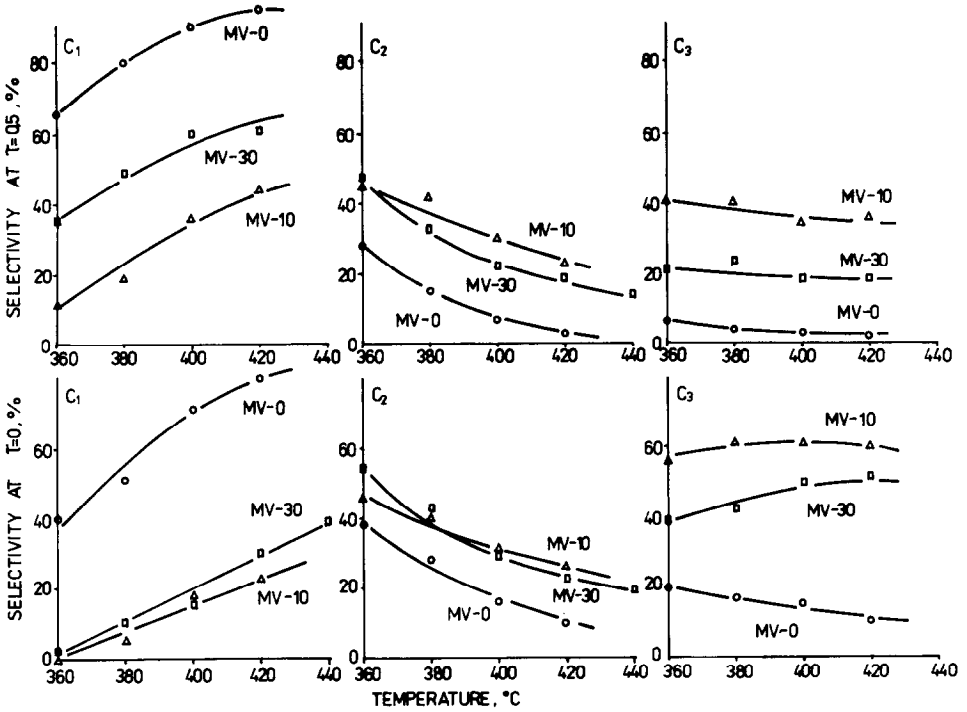

FIG. 9. (20$\bar{2}$) series of MV-X. Selectivities (σ) to C_1, C_2, and C_3 products at $\tau = 0$ and at $\tau = 0.5$ as function of temperature.

of this transformation has been the subject of many studies which have been reviewed and commented on widely by Dadyburjor *et al.* (*17*). There is general agreement that the mechanism involves the dissociative adsorption of propylene, formation of the π-allylic complex as an intermediate and successive incorporation of one or two oxygen atoms. Our results provide only some contribution regarding the incorporation of the second oxygen. The shape of the $Y-\tau$ curves (Fig. 8) for acrylic acid does not prove that it is formed as a product of the consecutive oxidation of acrolein. On the contrary, a certain initial selectivity to acrylic acid is observed. This would suggest that propylene adsorbed on a K_3 center (see Fig. 12a) and initially oxidized to an acrolein-like surface intermediate may incorporate the second oxygen on the same center, without desorption.

As follows from Figs. 6 and 9, Y_3 increases with temperature while σ_3, being nearly temperature independent, strongly decreases with contact time. This suggests that (1) the changes of σ_1 and σ_2 with temperature compensate one another, this effect being possible if the majority of the C_1 products is formed on a K_2 center and only a litle on K_1, (2) the activation energy of C_3 formation should be close to that of C_3 consecutive combustion, and (3) since the oxidation of propylene is initiated alternatively on K_2 and K_3 centers and the ratio $\sigma_3/(\sigma_1 + \sigma_2)$ is nearly temperature independent, the activation energies of the processes taking place on the two active centers should be comparable.

The above-described mechanism of the oxidation of propylene on the (20$\bar{2}$) plane of MV-X solid solutions is summarized in Fig. 12a. The presence of at least two types of active centers able to incorporate in "one stage" (i.e., without desorption) more than one oxygen atom to the molecule of propylene (or to the products of its degradation) is the characteristic feature of this plane. The results obtained provide no precise infor-

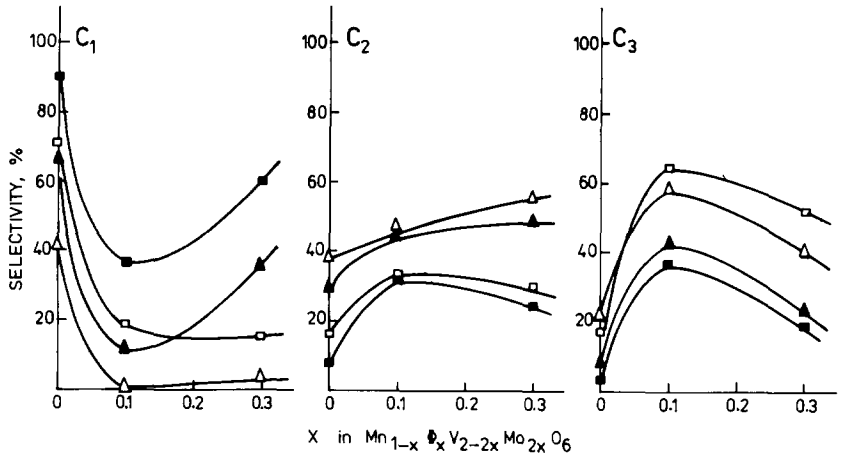

FIG. 10. (20$\bar{2}$) series of MV-X. Selectivities (σ) to C_1, C_2, and C_3 products as a function of composition parameter x. Squares, 400°C; triangles, 360°C; open symbols, $\tau = 0$; solid symbols, $\tau = 0.5$.

mation about the nature of K_1 centers. It may not, however, be excluded that they are identical with K_2 centers.

(201) Series of MV-X Catalysts

The results of the catalytic testing of the (201) series are presented in Figs. 4, 7, and 11. Comparing them with those of the (20$\bar{2}$) series one may easily note a strong decrease of Y_1, a medium decrease of Y_2, and a small decrease of Y_3. Finally, the (201) preparations are several times less active than the (20$\bar{2}$) samples.

MV-0 is the only catalyst of the (201) series for which $\sigma_1^0 > 0$. Moreover, acrolein and acetaldehyde are efficiently combusted in consecutive reactions and the respective acids are never observed among the products. On the contrary, as can be seen from the shape of the $Y-\tau$ curves (Fig. 7) recorded for doped preparations, the oxidation of propylene passes through two parallel reaction branches along which three- and two-carbon containing aldehydes and acids are consecutively formed and finally transformed to the C_1 products. In particu-

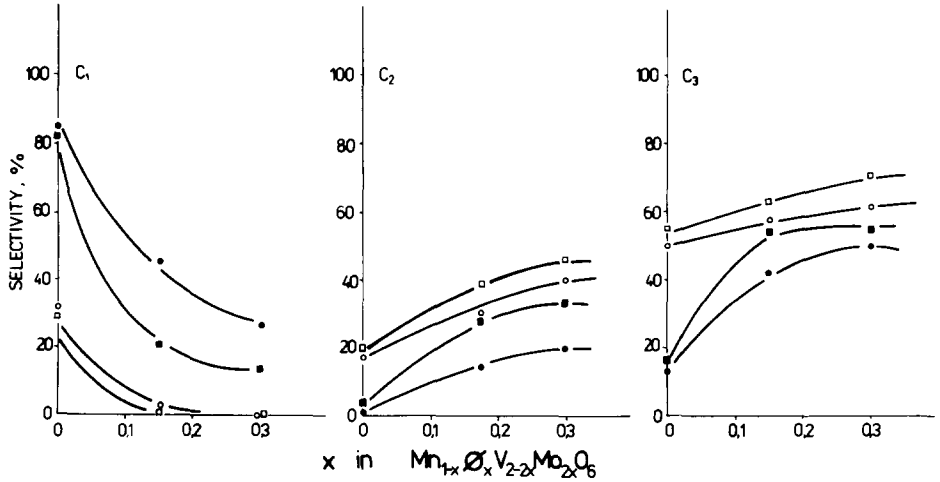

FIG. 11. (201) series of MV-X. Selectivities (σ) to C_1, C_2, and C_3 products as a function of composition parameter x. Circles, 440°C; squares, 400°C; open symbols, $\tau = 0$; solid symbols, $\tau = 0.5$

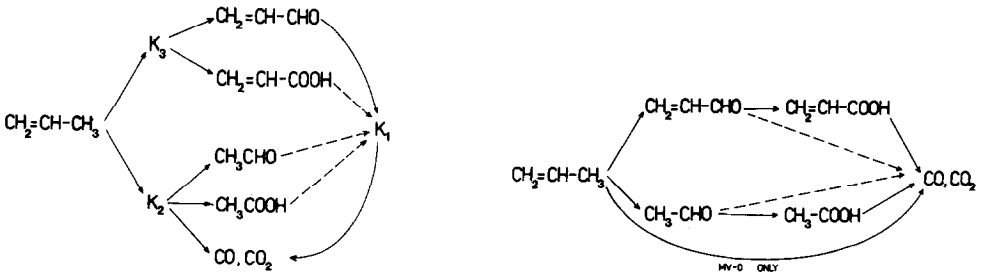

FIG. 12. Propylene oxidation schemes on (a) $(20\bar{2})$ and (b) (201) crystallographic planes of $Mn_{1-x}\phi_xV_{2-2x}Mo_{2x}O_6$ (MV-X) solid solutions. Full lines represent the efficient reactions, dotted lines represent presumed reactions.

lar this conclusion is based on the sigmoid shape of the $Y-\tau$ curves for acetic acid and acrylic acid and on the fact that both acids appear among the products only at longer contact time.

The reaction scheme for the (201) plane is summarized in Fig. 12b. It seems that on the (201) plane of MV-X catalysts there predominate the active centers able to effect the successive, one-by-one, incorporation of oxygen into the organic molecule, separated by the desorption–adsorption processes.

As regards the somewhat exceptional properties of the MV-0 sample, it is difficult to answer the question whether they really reflect the properties of the nondoped (201) plane, or to what extent they are influenced by the simultaneous presence of the nondoped $(20\bar{2})$ plane, known to be extremely active in total combustion. Evidently the presence of the latter plane may not be entirely eliminated in the case of three-dimensional grains. Due to the same reason the results obtained for the doped samples of the (201) series may be influenced to some extent by the simultaneous presence of the more active $(20\bar{2})$ plane, and thus the reaction scheme for the (201) plane seems to be somewhat less substantiated than that for the $(20\bar{2})$ plane.

Final Remarks

The results obtained suggest that the $(20\bar{2})$ face of MV-X catalysts must contain the active centers surrounded by several active oxygen atoms. On the contrary, the active oxygens on the (201) plane should be predominantly separated. The common feature of both planes is a total combustion which is vastly diminished on increase of the composition parameter x. The last observation remains in agreement with the preliminary stepwise thermodesorption experiments which have shown that the MV-0 sample contains at its surface a relatively large amount of loosely bound oxygen desorbing at 200–400°C as compared with the highly doped sample releasing oxygen mainly at 400–500°C.

The abovementioned properties must result from the differences in the $(20\bar{2})$ and (201) plane structure and its modification on doping. The analysis of these structures has been undertaken and the conclusions will be reported in a forthcoming paper.

ACKNOWLEDGMENTS

The authors wish to thank Miss Krystyna Krupa for assistance in part of the catalytic work and Dr. Antonina Kozłowska for the preliminary thermodesorption examination. We are also indebted to Professor Jerzy Haber for his interest and encouragement during the course of the investigations.

Scanning electron microscopy observations were performed in the Regional Laboratory of Physicochemical Analyses and Structural Research in Kraków.

REFERENCES

1. Stone, F. S., *in* "Chemical and Physical Aspects of Catalytic Oxidation" (J. L. Portefaix and F. Figueras, Eds.), p. 459 (Ecole de Printemps,

Lyon-Ecully 1978). Editions C.N.R.S., Paris, 1980.
2. Sleight, A. W., *in* "Advanced Materials in Catalysis" (J. J. Burton and R. L. Garten, Eds.), p. 181. Academic Press, New York, 1977, and papers cited therein.
3. Ruh, R., and Wadsley, A. D., *Acta Crystallogr.* **21,** 974 (1966).
4. Ng, H. N., and Calvo, C., *Canad. J. Chem.* **50,** 3619 (1972).
5. Kozłowski, R., Ziółkowski, J., Mocała, K., and Haber, J., *J. Solid State Chem.* **35,** 1 (1980); erratum **38,** 138 (1981).
6. Bouloux, J. C., and Galy, J., *Bull. Soc. Chim. Fr.* 736 (1969).
7. Angenault, J., *Rev. Chim. Miner.* **7,** 651 (1970).
8. Gondrad, M., Collomb, A., Joubert, J. C., and Shannon, R. D., *J. Solid State Chem.* **11,** 1 (1974).
9. Calvo, C., and Manolescu, D., *Acta Crystallogr. B* **29,** 1743 (1973).
10. Ziółkowski, J., Kozłowski, R., Mocała, K., and Haber, J., *J. Solid State Chem.* **35,** 297 (1980).
11. Machej, T., Kozłowski, R., and Ziółkowski, J., *J. Solid State chem.* **38,** 97 (1981).
12. Galy, J., Darriet, J., and Darriet, B., *C.R. Acad. Sci. Paris Ser. C* **264,** 1477 (1967).
13. Mocała, K., and Ziółkowski, J., in preparation.
14. Volta, J. C., Desquesnes, W., Moraweck, B., and Tatibouët, J. M., Proc. Int. Congr. Catalysis, 7th (Tokyo 1980), p. 1398. Elsevier, Amsterdam, 1981.
15. Figueras, F., Figlarz, M., Portefaix, J. L., Forissier, M., Gerand, B., and Guenot, J., *J. Catal.* **71,** 389 (1981).
16. Kozłowski, R., and Stadnicka, K., *J. Solid State chem.* **39,** 271 (1981).
17. Dadyburjor, D. B., Jewur, S. S., and Ruckenstein, E., *Catal. Rev. Sci. Eng.* **19,** 293 (1979).